ELSEVIER

Materials Science and Engineering A239–240 (1997) 393–398

MATERIALS SCIENCE & ENGINEERING A

Laminated Nb/Nb_3Al composites: effect of layer thickness on fatigue and fracture behavior

D.R. Bloyer [a], K.T. Venkateswara Rao [b], R.O. Ritchie [a,*]

[a] Department of Materials Science and Mineral Engineering, University of California at Berkeley, Berkeley, CA 94720-1760, USA
[b] Guidant Corporation, Advanced Cardiovascular Systems, 3200 Lakeside Dr., P.O. Box 58167, Santa Clara, CA 95052, USA

Abstract

Fracture and fatigue crack growth properties of coarse scale Nb/Nb_3Al laminated composites are examined, and their performance is contrasted with similarly reinforced in situ particulate and microlaminate composites. It is found that laminate orientation has a larger effect on fatigue crack growth resistance than on fracture toughness; properties are optimal in the crack arrester as compared with the crack divider orientation. In addition, thicker Nb layers yield improved fracture and fatigue crack growth properties; and the effect is more prominent in the divider orientation. Mechanisms underlying this behavior are briefly described. © 1997 Elsevier Science S.A.

Keywords: Fracture; Fatigue; *R*-curve; Intermetallic; Nb; Nb_3Al; Laminates

1. Introduction

Intermetallic alloys have generated increasing interest over the past decade as possible replacements for titanium- and nickel-based superalloys currently used in aerospace applications. Attractive properties include higher melting temperatures and lower densities which provide improved specific creep strength for elevated temperature structures in high performance engines [1]. However, as most intermetallic compounds are brittle due to their ordered crystal structure, they generally suffer from poor room-temperature fracture resistance. To improve their low intrinsic toughness, extrinsic toughening techniques that invoke crack-tip shielding mechanisms are often used in alloy design and microstructural development. Such mechanisms, which include crack bridging via ductile or brittle reinforcements, primarily act behind the crack tip and locally screen the crack from the applied far field driving force [2,3]. Examples of materials toughened in this manner are various ceramic- and intermetallic-matrix composites, such as Co/WC, Al/Al_2O_3, $Nb/MoSi_2$, Al or Mg/glass, Nb or TiNb/TiAl, Mo or Cr/NiAl, and Nb/Nb_3Al, that incorporate ductile (or brittle) reinforcements in the form of particulates [4–6], fibers [7–9], or laminates [10–23]. Despite such efforts in improving the toughness of brittle materials using ductile metal reinforcements, work in several intermetallic systems (e.g. [13]) has shown that the toughening induced by the ductile phase can be severely degraded under cyclic loading, which will likely be present in many structural applications.

In the present study, we examine the fracture and fatigue behavior of a model Nb-reinforced Nb_3Al composite, where toughening is achieved by the addition of ductile Nb layers having layer dimensions in the tens to hundreds of microns. Results are compared with earlier studies which involved Nb/Nb_3Al composites with Nb as ~ 20 μm particulate reinforcement fabricated in situ by powder metallurgy [6], or as 2 μm thick (magnetron sputtered) layers to form a microlaminate [20].

2. Experimental procedures

Two laminate orientations were investigated in this study, namely the 'crack arrester' (0° or C-L), where the crack grows perpendicular to, yet sequentially through, the layers (Fig. 1(a)), and the 'crack divider' (C-R), where the crack plane is normal to the plane of layers,

* Corresponding author.

0921-5093/97/$17.00
PII S0921-5093(97)00608-4

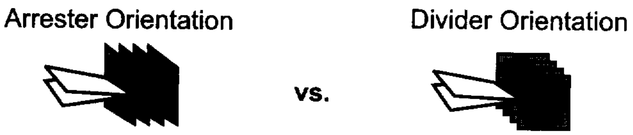

Fig. 1. Laminate orientation.

but the crack advances through all the layers simultaneously (Fig. 1(b)). To study the effect of laminate thickness, composites with layer thicknesses of 50 μm Nb/200 μm Nb_3Al, 125 μm Nb/500 μm Nb_3Al, and 250 μm Nb/1000 μm Nb_3Al were prepared by cold compacting Nb_3Al powder between Nb foils. The compacts were then hot pressed between 1500 and 1680°C in an argon atmosphere to give dense composite cylinders with nominally 20 vol.% Nb reinforcements. Some reaction did occur between the Nb and the intermetallic resulting in an effective reduction of reinforcement volume fraction to ∼16%, ∼14–15%, ∼17% for the 50, 125 and 250 μm Nb laminates, respectively.

Single-edged notched bend beams having widths, W, of 9.5, 12.5 and 13.3 mm for the 50, 125, and 250 μm Nb laminates, respectively, were used to study the resistance curve (R-curve) and fatigue behavior of the arrester orientation for all layer thicknesses. The exception was the 125 μm Nb laminate where compact tension specimens with $W = 25.4$ mm were used. Divider fracture and fatigue testing were performed using disc compact tension specimens with $W = 33$ mm for all layer thicknesses.

3. Results and discussion

3.1. R-curve behavior

The R-curves, plotted in Fig. 2 for the divider orientation, illustrate that the addition of high aspect ratio ductile reinforcements leads to significant improvements in the fracture behavior of Nb_3Al. Compared with the intrinsic toughness of only ∼1 MPa$\sqrt{m}$ for monolithic Nb_3Al, the addition of 20 vol.% of 50 μm thick Nb layers resulted an initiation toughness of ∼5 MPa$\sqrt{m}$ and a maximum toughness (on the R-curve) exceeding 10 MPa$\sqrt{m}$. The 125 and 250 μm Nb laminates yielded even better properties having initiation toughnesses of 6.7 and 7.1 MPa$\sqrt{m}$, respectively, and corresponding maximum toughnesses over 15 and 20 MPa$\sqrt{m}$. The high toughness achieved by these laminates is a result of crack tunneling in the intermetallic phase between the Nb layers. It was observed that cracks tunneled ahead in the Nb_3Al matrix almost the entire crack growth range leaving extensive bridging zones behind the crack tip to shield the far-field applied stress intensity.

Even though the present laminates contain only 20 vol.% Nb, they exhibit higher toughness than Nb particulate toughened Nb_3Al composites containing twice as much Nb [6] (Fig. 2(b)). Moreover, they display comparable or superior toughness to microlaminates consisting of 50 vol.% of ∼2 μm thick Nb layers in Nb_3Al, which have initiation and steady-state toughnesses of only 6 and 10 MPa$\sqrt{m}$, respectively [20]. For the latter material, quasi-static crack extension occurred only over the first 200 μm of growth; in contrast, the present laminates exhibited stable cracking over crack

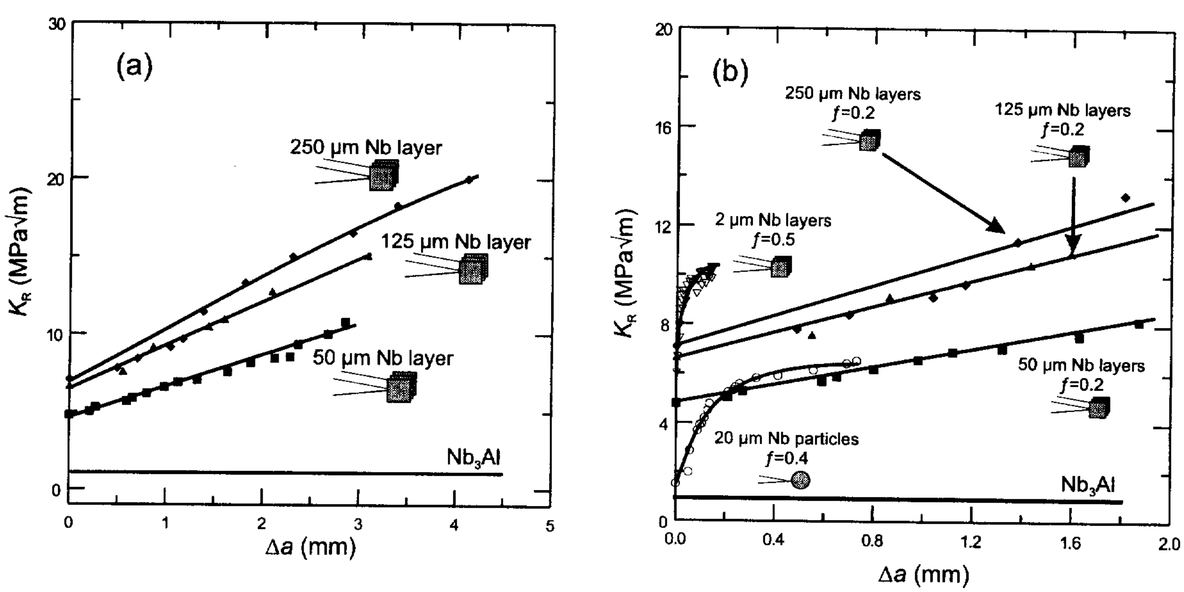

Fig. 2. (a) Divider orientation R-curves; (b) magnified region of (a).

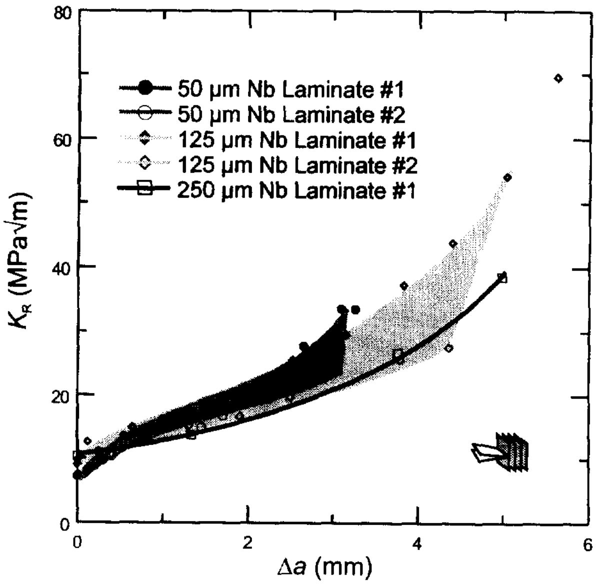

Fig. 3. Arrester orientation R-curves.

extensions of 3 mm or more. It is clear that the laminates with coarser Nb layers require far less reinforcement to achieve equivalent or superior fracture toughness properties; indeed, compared with particulate or microlaminate reinforcement, the crack initiation toughness, the maximum crack growth toughness, and the extent of subcritical cracking prior to instability are generally all enhanced.

Consistent with prior studies [17], the initiation toughness did steadily increase with layer thickness for the arrester orientation (Fig. 3) with values of ~7.3, 9 and 10.4 MPa$\sqrt{m}$ for the 50, 125 and 250 μm thick Nb layers, respectively. The maximum toughness was ~20 MPa$\sqrt{m}$ or more for all layer thicknesses and was generally higher than that of the divider laminates for a given reinforcement layer thickness. Extensive bridging was also responsible for the significant improvement in maximum toughness of the arrester laminates. The 50 μm Nb and 125 μm laminate appeared to just reach equilibrium bridging zone sizes of ~3 and ~5 mm, respectively, but the 250 μm laminate crack showed no sign of an equilibrium zone length and remained fully bridged.

Large scale bridging (LSB) conditions—when the bridging zone is large relative the crack length and the uncracked ligament—are expected to apply to the laminates in both orientations due to the limited sample sizes and the large bridging zones. LSB causes the R-curve to become geometry dependent [14,24], but modeling techniques do allow predictions of small scale bridging R-curve behavior to be extracted from the measured R-curves, as shown below.

The stress intensity reduction caused by the shielding tractions in the bridging zone of these composites can be calculated using weight function methods [25], specifically Green's functions, that allow the shielding stress intensity to be obtained for any form of the traction function. This shielding contribution can then be superposed with some intrinsic toughness of the composite, and the applied stress intensity, K_{app}, for a given loading condition can be predicted by:

$$K_{app} = K_0 + \int_L \sigma(x) h(a, x)\, dx \qquad (1)$$

where K_0 is the initiation toughness of the composite, L is the bridging zone length, $\sigma(x)$ is the traction as a function of distance behind the crack tip, $h(a, x)$ is the weight function, and the integration limits are determined by the bridging zone length.

A simplified approach to this problem was to assume that $\sigma(x)$ is a constant function $f\sigma_c$, where σ_c is the constrained flow stress and f is the reinforcement volume fraction [8]. Earlier studies on Nb in $MoSi_2$ [19] and Nb in Nb_5Si_3 [18] indicate this is a reasonable assumption for these composites as the constrained load-displacement curves for Nb laminates rise rapidly to relatively constant plateaus with continuing displacement.

Using Eq. (1) and the appropriate bridging zone lengths, the arrester R-curves were fit to obtain the effective constrained flow stress, σ_c, for each laminate thickness combination. Average constrained flow stress values of 370, 490 and 540 MPa were obtained for the 250, 125 and 50 μm Nb laminates, respectively. These values for constrained flow stress are consistent with values found in previous studies of constrained metal layers [7,11,19] that gave numbers ranging from one to seven times the uniaxial flow stress of the unconstrained metal layer. In addition, a value of 370 MPa for the 250 μm Nb laminate compares very well to the measurement of ~400 MPa found by Pickard and Ghosh [19] for a 250 μm Nb layer in $MoSi_2$.

These constrained yield stresses can be used in a small scale bridging model based on an energy approach where the reinforcement toughening contribution, $G_b = f\sigma_0 t\chi$ [7] can be superposed with the matrix fracture energy (and ignoring cross terms) to give an expression for the composite toughness [7]:

$$K_{ss} = \sqrt{K_0^2 + E' f \sigma_0 t \chi} \qquad (2)$$

where K_{ss} is the steady-state (or plateau) toughness, and K_0 is the crack-initiation toughness.

To evaluate Eq. (2), we set the constrained flow stress equal to $\chi\sigma_0$, the nondimensional work of rupture times the unconstrained flow stress, and substitute f, the half layer thickness, t, and plane-strain composite modulus, E' (all corrected for the reaction layer) to calculate steady state small scale yielding stress intensities. Predicted values of 17, 22 and 33 MPa$\sqrt{m}$ were calculated for the 50, 125 and 250 μm Nb laminates, respectively,

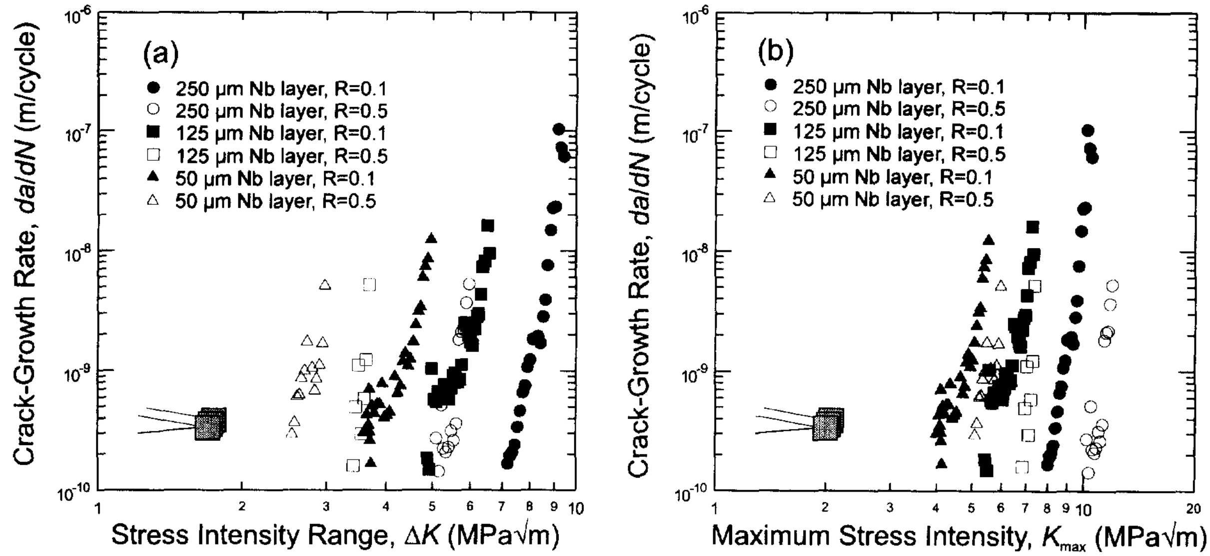

Fig. 4. Divider fatigue curves plotted (a) against ΔK (b) against K_{max}.

from the constrained flow stresses obtained in the above bridging analysis. These maximum toughness values are reasonably consistent with the measured R-curves (Fig. 3), except for the 250 μm Nb laminate where the R-curve shape was significantly altered by the LSB conditions.

3.2. Fatigue behavior

Results presented in Figs. 4 and 5 show that the addition of Nb as a laminated phase in either orientation dramatically increases the fatigue crack growth resistance of the Nb_3Al intermetallic, specifically, crack growth rates are improved by 3–7 MPa$\sqrt{m}$, depending on the composite layer thickness and orientation. Fatigue thresholds are enhanced by ~133–233% using the high aspect ratio reinforcing layers (Fig. 4(a)). This demonstrates that the laminates are far more resistant to the cyclic loading induced degradation in shielding than the Nb particulate reinforced Nb_3Al composites examined earlier [6]. It should again be noted that these improvements have been achieved using a reinforcement volume fraction which is half that of the particulate composite. Based upon these comparisons, laminate reinforcements are clearly the best choice for improving the fatigue crack growth properties of brittle materials when forming composites by the incorporation of a ductile second phase.

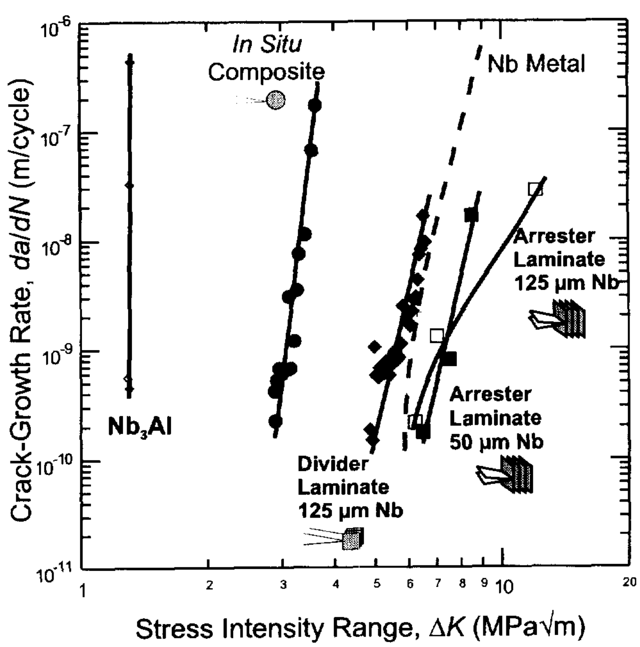

Fig. 5. Arrester fatigue curves.

The arrester orientation yielded a fatigue threshold of ~6.5 MPa$\sqrt{m}$ that was essentially independent of laminate thickness; indeed, thresholds in this orientation were generally higher than in the divider orientation. However, the fatigue cracking growth rates in the arrester laminates decreased with increasing Nb layer thickness, implying improved fatigue crack growth resistance. The arrester laminates showed a fatigue threshold which was very similar to that observed for the Nb metal, processed under similar conditions (Fig. 5). The slope change of the fatigue curves appeared to be closely related to the change in crack-layer interactions with increasing applied stress intensity range. Metallograhic investigations revealed that at lower ΔK levels the crack impinges on the Nb reinforcing layer and proceeds to fatigue through the metal layer prior to renucleation in the Nb_3Al intermetallic. As a result, bridging ligaments in the crack wake become evanescent, and the fatigue threshold of the arrester laminates

Table 1
Power law exponents, n and p (Eq. (3)), for divider laminates

Nb/Nb_3Al layer thickness	50 μm Nb/200 μm Nb_3Al	125 μm Nb/500 μm Nb_3Al	250 μm Nb/1000 μm Nb_3Al
n	3	3	10
p	7	8	13

appeared to be dominated by the Nb metal fatigue properties. In contrast, higher applied ΔK levels caused crack renucleation in the Nb_3Al across the Nb layer and the subsequent development of a bridging zone behind the crack tip because the maximum applied stress intensity approaches or exceeds the monotonic crack initiation toughness [23]. This bridging zone then acted to shield the crack tip and improved crack growth properties.

Fig. 4(a) also shows that there was a significant improvement in the fatigue crack resistance of the divider orientation with increasing reinforcement layer thickness. Fatigue thresholds increased from ~3.5 to 5 to 7 MPa$\sqrt{m}$ for the 50, 125 and 250 μm Nb laminates, respectively, at a load ratio of 0.1. Higher mean stresses, achieved using a load ratio of 0.5, appear to degrade the cyclic crack growth resistance of these composites and reduce the thresholds by about 30% to 2.5, 3.5 and 5 MPa$\sqrt{m}$, respectively. Replotting the fatigue data in terms of K_{max} (Fig. 4(b)) narrows the spread of the data with respect to mean stress variation, indicating that the monotonic fracture mechanism of the brittle Nb_3Al intermetallic has a significant influence on the cyclic crack growth process. However, neither ΔK nor K_{max} completely normalizes the load ratio effect, similar to behavior in other intermetallics [9]. This is supported by fitting the fatigue curves to a modified Paris equation [26]:

$$\frac{da}{dN} \propto \Delta K^{n} \cdot K_{max}^{p} \quad (3)$$

where the exponents for each layer thickness, given in Table 1, are comparable, unlike in metals (where $n \gg p$) and ceramics ($p \gg n$).

Bridging zones of ~1, 3 and 5 mm for the 50, 125 and 250 μm Nb laminates, respectively, were observed during the decreasing ΔK tests. The bridges resulted from crack tunneling and are believed to be responsible for the improved fatigue crack growth resistance observed as the laminate thickness increased.

4. Conclusions

Based on a study of the fracture and fatigue behavior of the Nb reinforced Nb_3Al laminates, the following conclusions can be made:

- Dramatic improvements in monotonic and cyclic crack growth resistance of brittle Nb_3Al intermetallics can be achieved using significantly lower volume fractions of ductile Nb reinforcements as coarse (50–250 μm) laminates compared with particulates or microlaminates (2 μm layers); toughness improvements of 10–20 times that of the brittle Nb_3Al matrix and two to three times that of a particulate reinforced Nb/Nb_3Al composite were readily achieved. Similar improvements in fatigue threshold of four to seven times and 1.3–2.3 times that of the matrix and particulate composites, respectively, were observed.
- The effect of laminate orientation was more significant for fatigue crack growth than for monotonic toughness, with the arrester laminates generally showing improved properties over the divider laminates.
- Increasing the layer thickness improves both fracture toughness and fatigue-crack growth resistance of Nb/Nb_3Al laminates. However, the influence of coarsening the scale of Nb reinforcement was far more apparent in the crack-divider than the crack arrester orientation.

Acknowledgements

This work was supported by the US Air Force Office of Scientific Research under the AASERT Program, Grant No. F49620-93-1-0441, as a supplement to Grant No. F49620-93-1-0107.

References

[1] D.L. Anton, D.M. Shah, in: C.T. Liu et al. (Eds.), High Temperature Ordered Intermetallic Alloys III, MRS Symp. Proc. 133, Materials Research Society, Pittsburgh, PA, 1989, p. 361.
[2] A.G. Evans, J. Am. Ceram. Soc. 72 (1990) 187.
[3] R.O. Ritchie, Mater. Sci. Eng. A103 (1988) 15.
[4] L.S. Sigl, P.A. Mataga, B.J. Dalgleish, R.M. McMeeking, A.G. Evans, Acta Metall. 36 (1988) 945.
[5] K.T. Venkateswara Rao, W.O. Soboyejo, R.O. Ritchie, Metall. Trans. 23A (1992) 2249.
[6] C.D. Bencher, A. Sakaida, K.T. Venkateswara Rao, R.O. Ritchie, Metall. Mater. Trans. 26A (1995) 2027.
[7] M.F. Ashby, F.J. Blunt, M. Bannister, Acta Metall. 37 (1989) 1847.
[8] F. Zok, C.L. Hom, Acta Metall. Mater. 38 (1990) 1895.

[9] K. Badrinarayanan, A.L. McKelvey, K.T. Venkateswara Rao, R.O. Ritchie, Metall. Mater. Trans. 27A (1996) 3781.
[10] H.E. Dève, A.G. Evans, G.R. Odette, R. Mehrabian, M.L. Emiliani, R.J. Hecht, Acta Metall. Mater. 38 (1990) 1491.
[11] M. Bannister, M.F. Ashby, Acta Metall. Mater. 39 (1991) 2575.
[12] K.T. Venkateswara Rao, G.R. Odette, R.O. Ritchie, Acta Metall. Mater. 40 (1992) 353.
[13] K.T. Venkateswara Rao, G.R. Odette, R.O. Ritchie, Acta Metall. Mater. 42 (1994) 893.
[14] G.R. Odette, B.L. Chao, J.W. Sheckhard, G.E. Lucas, Acta Metall. Mater. 40 (1992) 2381.
[15] F.E. Heredia, M.Y. He, G.E. Lucas, A.G. Evans, H.E. Dève, D. Konitzer, Acta Metall. Mater. 41 (1993) 505.
[16] M.Y. He, F.E. Heredia, D.J. Wissuchek, M.C. Shaw, A.G. Evans, Acta Metall. Mater. 41 (1993) 1223.
[17] M.C. Shaw, D.B. Marshall, M.S. Dadkhah, A.G. Evans, Acta Metall. Mater. 41 (1993) 3311.
[18] J. Kajuch, J. Short, J.J. Lewandowski, Acta Metall. Mater. 43 (1995) 1955.
[19] S.M. Pickard, A.K. Ghosh, Metall. Mater. Trans. 27A (1996) 909.
[20] J. Heathcote, G.R. Odette, G.E. Lucas, Acta Mater. 44 (1996) 4289.
[21] D.R. Bloyer, K.T. Venkateswara Rao, R.O. Ritchie, Mater. Sci. Eng. A216 (1996) 80.
[22] D.R. Bloyer, K.T. Venkateswara Rao, R.O. Ritchie, in: R.J. Arsenault et al. (Eds.), Johannes Weertman Symposium, TMS, Warrendale, PA, 1996, p. 261.
[23] D.R. Bloyer, K.T. Venkateswara Rao, R.O. Ritchie, in: J.J. Lewandowski et al. (Eds.), Layered Materials for Structural Applications, MRS Symp. Proc. 434, Materials Research Society, Pittsburgh, PA, 1996, p. 243.
[24] B.N. Cox, C.S. Lo, Acta Metall. Mater. 40 (1992) 69.
[25] T. Fett, D. Munz, G. Thun, H.A. Bahr, J. Am. Ceram. Soc. 78 (1995) 949.
[26] R.H. Dauskardt, M.R. James, J.R. Porter, R.O. Ritchie, J. Am. Ceram. Soc. 75 (1992) 759.